Inorganic Chemistry

Article

pubs.acs.org/IC

Large-Scale Synthesis of Monodisperse Magnesium Ferrite via an Environmentally Friendly Molten Salt Route

Zhengsong Lou,*[,†,‡] Minglong He,[†] Ruikun Wang,[‡] Weiwei Qin,[†] Dejian Zhao,[†] and Changle Chen*[,‡]

[†]Jiangsu Key Laboratory of Precious Metals Chemistry and Engineering, School of Chemistry and Environment Engineering, Jiangsu University of Technology, Changzhou 213001, P. R. China

[‡]CAS Key Laboratory of Soft Matter Chemistry, Department of Polymer Science and Engineering, University of Science and Technology of China, Hefei, 230026, China

ABSTRACT: Sub-micrometer-sized magnesium ferrite spheres consisting of uniform small particles have been prepared using a facile, large-scale solid-state reaction employing a molten salt technique. Extensive structural characterization of the as-prepared samples has been performed using scanning electron microscope, transmission electron microscopy, high-resolution transmission electron microscopy, selected area electron diffraction, and X-ray diffraction. The yield of the magnesium ferrite sub-micrometer spheres is up to 90%, and these sub-micrometer spheres are made up of square and rectangular nanosheets. The magnetic properties of magnesium ferrite sub-micrometer spheres are investigated, and the magnetization saturation value is about 24.96 emu/g. Moreover, the possible growth mechanism is proposed based on the experimental results.

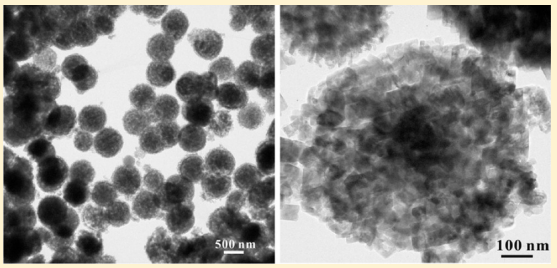

INTRODUCTION

Monodisperse nano-/microspheres exhibit a variety of unique properties, making them suitable for many potential uses.[1−6] For example, their applications have been demonstrated in optical and photonic crystals,[7,8] sensors,[9,10] colloidal lithography,[11] porous membranes,[12,13] seed particles for the core−shell and hollow spheres,[3,14] catalyst support,[15] etc. As a result, novel synthetic strategies have been intensively pursued.

Monodisperse nanostructured magnetic materials have attracted much attention due to their unique magnetic features and important applications as advanced magnetic materials, catalysts, colored pigments, high-density magnetic recording media, drug delivery, and cancer detection.[16−25] Magnesium ferrite ($MgFe_2O_4$), as a soft magnetic *n*-type semiconducting material, is an important member of the spinel family. Apart from magnetic and electronic applications, it has been widely applied in heterogeneous catalysis, adsorption[26,27] and sensor technology.[28−30]

Monodisperse ferrite materials can be prepared by various methods, such as coprecipitation, reverse micelle method, ultrasound irradiation, hydrothermal method, laser pyrolysis techniques, thermal decomposition of organometallic compounds.[31−37] However, most of these methods require multiple steps and handling of large amounts of organic reagents, solvents and surfactants, which raises synthetic costs and causes environmental pollution, making them not suitable for large-scale applications. Molten salt synthesis (MSS) is one of the simplest, most versatile, environmentally friendly, and cost-effective routes for the synthesis of crystalline, pure, and single-phase powders.[38] Recently, MSS has been demonstrated to prepare nanomaterials with different morphologies.[39] Herein, we report the preparation of monodisperse magnesium ferrite crystalline microspheres through MSS using NaCl and KCl molten salt at 800 °C. NaCl and KCl were chosen because they are cheap, harmless to human beings and the environment, and easily removed from the final products. More important, they provide a favorable growth environment for the magnesium ferrite.

EXPERIMENTS

Stoichiometric amounts of $Fe(NO_3)_3$, $Mg(NO_3)_2$, NaCl, and KCl were mixed (in molar ratios of 2:1:30*M*:10*M*, $0 < M < 7$, for generation of varying structural motifs), thoroughly ground in an agate mortar. In a typical synthesis, 2 mmol of $Fe(NO_3)_3$ and 1 mmol of $Mg(NO_3)_2$ along with 90 mmol of NaCl and 30 mmol of KCl were mixed thoroughly. The mixture was ground for at least 30 min. The processed mixture was ultimately placed in a ceramic crucible, inserted into a quartz tube, heated at a ramp rate of 5 °C per minute up to an annealing temperature at 800 °C for 4 h, and cooled thereafter to room temperature. The as-prepared material was washed several times with distilled water, collected by centrifugation, and dried at 80 °C overnight in a drying oven.

CHARACTERIZATION

The X-ray diffraction (XRD) analysis was performed using a Rigaku (Japan) D/max-γA X-ray diffractometer equipped with graphite monochromatized Cu Kα radiation (λ = 1.54178 Å). The morphology and the size distribution of the samples were investigated by scanning electron microscopy (SEM) with a Hitachi S-5200 microscope operating at 30 kV. The morphology of the samples and energy dispersive X-ray analysis (EDX) were taken on a field emission

Received: October 9, 2013
Published: January 31, 2014

dx.doi.org/10.1021/ic402558t | *Inorg. Chem.* 2014, 53, 2053−2057

scanning electron microscope (FESEM) (JEOL-6300F, 15 kV). Transmission electron microscopic (TEM) images were taken on a Hitachi H-800 transmission electron microscope. The microstructure of the samples and selected area electron diffraction (SAED) patterns were analyzed by high-resolution transmission electron microscopy (HRTEM), which was performed on a JEOL-2010 transmission electron microscope using an accelerating voltage of 200 kV. N_2 adsorption−desorption studies were carried out at 77 K with a static volumetric instrument Autosorb-1 (Quantachrome) to examine the porous properties of the sample. Samples were pretreated by outgassing in a vacuum at 200 °C for at least 5 h, and the pore size distribution was evaluated from the desorption isotherms using the BJH method. The magnetic properties of the products were investigated using a Physical Property Measurement System (Quantum Design, PPMS).

RESULTS AND DISCUSSION

The crystallinity and structure of the as-synthesized product were characterized by powder X-ray diffraction (PXRD). As shown in Figure 1, all diffraction peaks can be indexed to a

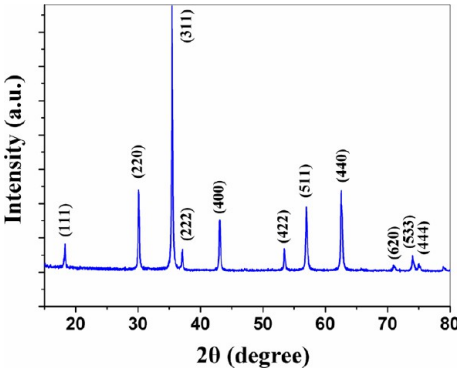

Figure 1. XRD pattern of the products.

cubic lattice, matching with standard *Fd*3*m* cubic spinel structured $MgFe_2O_4$ powder diffraction data (JCPDS 17-0464). The calculated lattice parameter is 8.375 Å, and no impurity phase can be found in the pattern.

The morphology of the product was examined by SEM and TEM. The obtained product is ubiquitous sub-micrometer spheres (more than 90% based on SEM analysis) with diameters ranging from 600 to 700 nm (Figure 2A,B). Nearly perfect spheres, broken spheres, and incomplete spheres with a rough surface can be clearly observed.

Energy dispersive spectrometry (EDS) analysis was utilized to determine the chemical composition of the magnesium ferrite sub-micrometer spheres. As shown in Figure 2C, the sample is composed of only magnesium, iron, copper, gold, and oxygen (copper and gold are coated on the surface of magnesium ferrite spheres to improve conductivity in SEM observations). No Na or K was observed, suggesting the efficient removal of the salts from the washing. The dynamic light scattering (DLS) results (Figure 2D) showed that the average hydrodynamic diameters of the spheres are about (650 ± 50) nm, which are consistent with the SEM results.

TEM image (Figure 3A) showed that the particles in the sample appear to be of nearly perfect spheres, and the sample contains large quantities of spheres range from 600 to 700 nm, which is in agreement with the result of SEM observation. In addition, a few small ones with a size of around 250 nm are also found present in the product. The spheres consisted of relatively uniform small particles, and the connecting interstices as shown in the enlarged TEM image (Figure 3B). Currently, we were not able to determine whether these small particles are thin flakes or small cubes. Most of the small particles are rectangular, with width ranging from 20 to 60 nm and length ranging from 50 to 200 nm. The SAED pattern (Figure 3C) contains six discernible diffraction rings, matching standard $MgFe_2O_4$ powder diffraction data. A more detailed investigation of as-prepared products was carried out by HRTEM. An HRTEM image of an individual small particle (Figure 3D) indicates an interplanar distance of 0.253 nm, which are characteristic of (311) spinel plane. The unique structures of these monodisperse magnetic sub-micrometer spheres make them potentially useful for selectively permeable capsules,[40] catalysis, drug-deliverym and advanced nanoelectronics.

The nitrogen adsorption isotherms of the magnesium ferrite sub-micrometer spheres obtained at 77 K are shown in Figure 4. The isotherms of the sample appears typically in Type IV characteristic, according to the IUPAC classification, with hysteresis loops initiating from the medium relative pressures ($P/P_0 \sim 0.40$) and closing near $P/P_0 \sim 1$. BJH cumulative desorption surface area is 73.54 $m^2\ g^{-1}$. The surface area is relatively high, which is in agreement with the HRTEM results. These results confirmed the porous nature of these sub-micrometer spheres.

Figure 5 shows the magnetization curves measured at 300 K. The magnetic saturation value was measured to be 24.96 emu/g, which is lower than that of bulk magnesium ferrite (about 26.9 emu/g)[41] and in accordance with the size determined saturation magnetization, and typical superparamagnetic 'S'-like shape of hysteresis loops was observed. Our results are consistent with that of Sun and co-workers and Chandradass and co-workers.[42] Detailed investigations of the magnetic properties of these products are in progress.

To investigate the effect of reaction conditions on the formation of magnesium ferrite sub-micrometer spheres, a series of control experiments were carried out. It was found that the amount of molten salt played a critical role in the formation of these sub-micrometer spheres. In a reaction at 800 °C without the addition of the NaCl and KCl molten salt, only amorphous magnesium ferrite was formed (Figure 6A), suggesting magnesium ferrite sub-micrometer spheres formation is related to the NaCl and KCl molten salts. At 800 °C, the reaction with 30 mmol of NaCl and 10 mmol of KCl produced random particulate (Figure 6B). The reaction using 60 mmol of NaCl and 20 mmol of KCl led to 50% of the magnesium ferrite sub-micrometer spheres (Figure 6C). As shown in Figures 2 and 3, the reaction using 90 mmol of NaCl and 30 mmol of KCl afforded a large amount of the magnesium ferrite sub-micrometer spheres. Interestingly, 150 mmol of NaCl and 50 mmol of KCl led to a mixture of flakes, spheres, and particles (Figure 6D). As the amount of molten salt was further increased, using 180 mmol of NaCl and 60 mmol of KCl as reactant, flakes became the major products (Figure 6E). Probably, it is simply a concentration issue. A higher $Fe(NO_3)_3$ and $Mg(NO_3)_2$ concentration (lower salt amount) leads to amorphous products, and a lower $Fe(NO_3)_3$ and $Mg(NO_3)_2$ concentration (higher salt amount) leads to flakes.

Reaction temperature also plays an important role. The reaction at 760 °C generated magnesium ferrite sub-micrometer spheres at 60% yield (Figure 6F). When the reaction was carried out at 860 °C, the yield of the magnesium ferrite sub-micrometer spheres was up to 75% (Figure 6G). At 900 °C, the main products were particulate and spheres (Figure 6H).

dx.doi.org/10.1021/ic402558t | Inorg. Chem. 2014, 53, 2053−2057

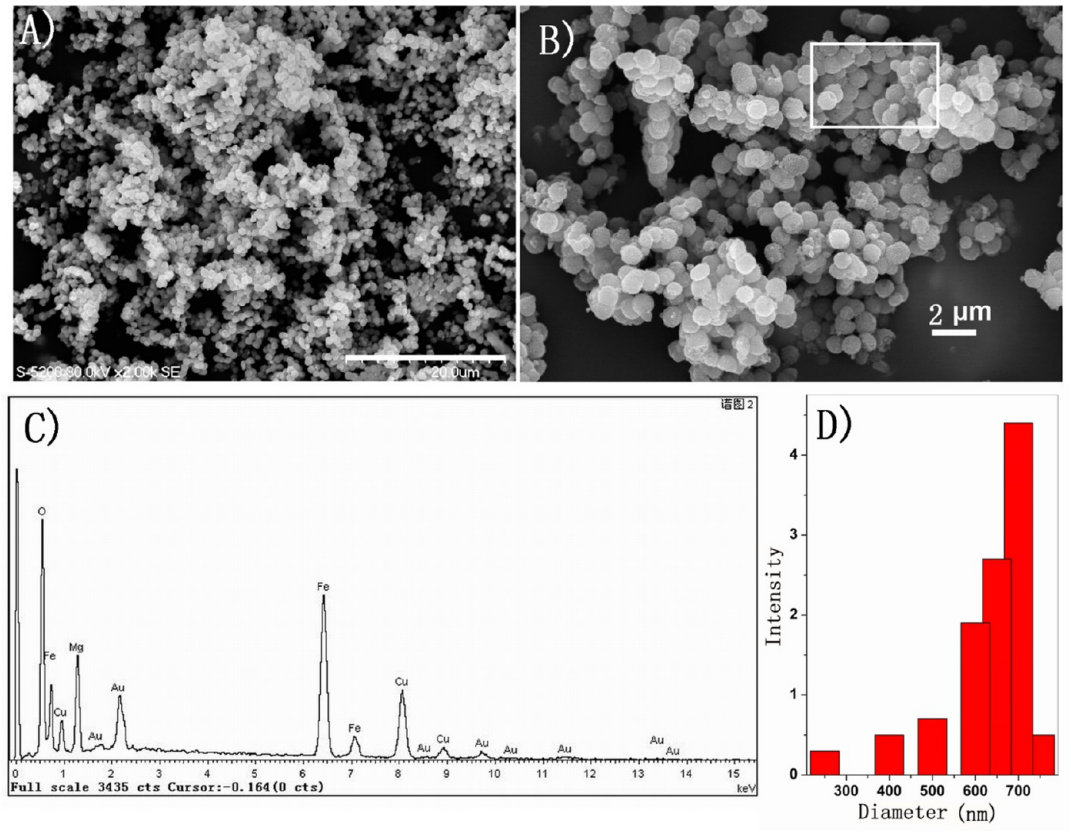

Figure 2. SEM image of the as-prepared product. (A) SEM image of sub-micrometer spheres and (B) the enlarged SEM image of sub-micrometer spheres shown in the rectangular area in (B). (C) EDS of magnesium ferrite spheres. (D) The dynamic light scattering size-distribution diagram.

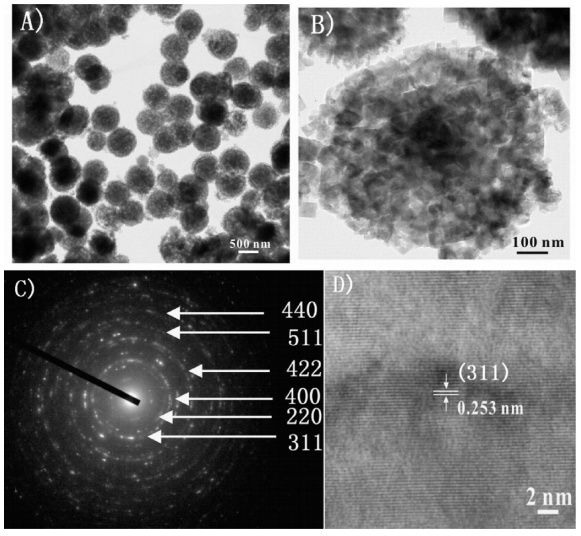

Figure 3. Images and electron diffraction pattern of the as-prepared sample taken on an HRTEM: (A) the typical TEM image; (B) the enlarged TEM image; (C) selected area electron-diffraction pattern; (D) HRTEM image.

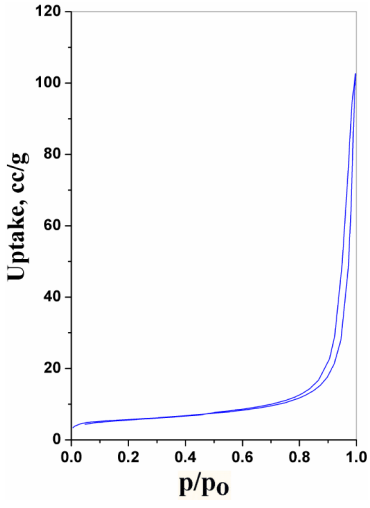

Figure 4. Nitrogen physisorption results of the magnesium ferrite sub-micrometer spheres: adsorption/desorption isotherms.

Reaction time also played a critical role in the synthesis. When the reaction was stopped after 180 min, ca. 60% of the sub-micrometer spheres were generated (Figure 6I). These results suggested that the growth of the sub-micrometer spheres is relatively slow. The influence of reaction conditions is summarized in Table 1. The average diameter of the sub-micrometer spheres can be tuned from 500 to 800 nm by varying the annealing temperature, time, and the amount of molten salt. In particular, the amount of molten salt played a critical role in the formation of these sub-micrometer spheres.

The melting point of NaCl and KCl is 805 °C and 774°, and the melting point of 3:1 NaCl−KCl mixture is 725 °C, according to the phase diagram of NaCl−KCl.[43] On the basis of our experimental results, possible growth mechanism was proposed. Upon heating of the initial mixture, the reactants were dissolved into the molten flux and gradually form $MgFe_2O_4$, which has limited solubility. As the concentration of $MgFe_2O_4$ increases, supersaturated solution was formed.

dx.doi.org/10.1021/ic402558t | Inorg. Chem. 2014, 53, 2053−2057

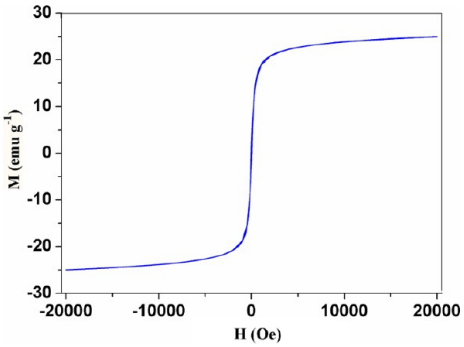

Figure 5. Magnetization curves of $MgFe_2O_4$ sub-micrometer spheres measured at 300 K.

Above the critical point, the initial nuclei of the cubic form can be generated.[44] Numerous magnesium ferrite small particles grow simultaneously. At high temperature (>750 °C), the thermal movement of the small particles leads to aggregation and eventually the formation of sub-micrometer solid sphere containing a small amount of molten salt. The molten salt is removed by treating with distilled water. Investigations on the detailed growth mechanism are still underway.

CONCLUSIONS

In summary, monodisperse magnesium ferrite sub-micrometer spheres consisting of rectangular small particles have been prepared on a large scale using a simple, one step solid-state chemical reaction in the presence of NaCl and KCl. The morphology of the product was investigated by SEM, TEM, and HRTEM. These monodisperse magnesium ferrite sub-micrometer spheres with unique structures may find applications in permeable capsules for drug delivery, catalysis, biomedicine, and biotechnology. Because of the simplicity, high yield, and green nature of this route, it may potentially be applied on large-scale industrial production. In addition, this

Table 1. $MgFe_2O_4$ Samples Systematically Prepared with Different Processing Parameters at a Constant Heating Rate of 5 °C/min

sample	annealing temperature/°C	NaCl and KCl molar ratio (30*M*:10*M*) M/mmol	time (min)	sample description (average particle size; morphology distribute)
A	800	0 (no salt)	240	no nanostructures
B	800	1	240	random particulate
C	800	2	240	600−750 nm spheres (50%)
expt cond	800	3	240	600−700 nm spheres (90%)
D	800	5	240	spheres (20%), flakes (60%), particles (20%)
E	800	6	240	flakes (80%)
F	760	3	240	500−700 nm spheres (70%)
G	860	3	240	600−800 nm spheres (75%)
H	900	3	240	700−800 nm spheres (10%), particulate (90%)
I	800	3	180	500−700 nm spheres (60%)

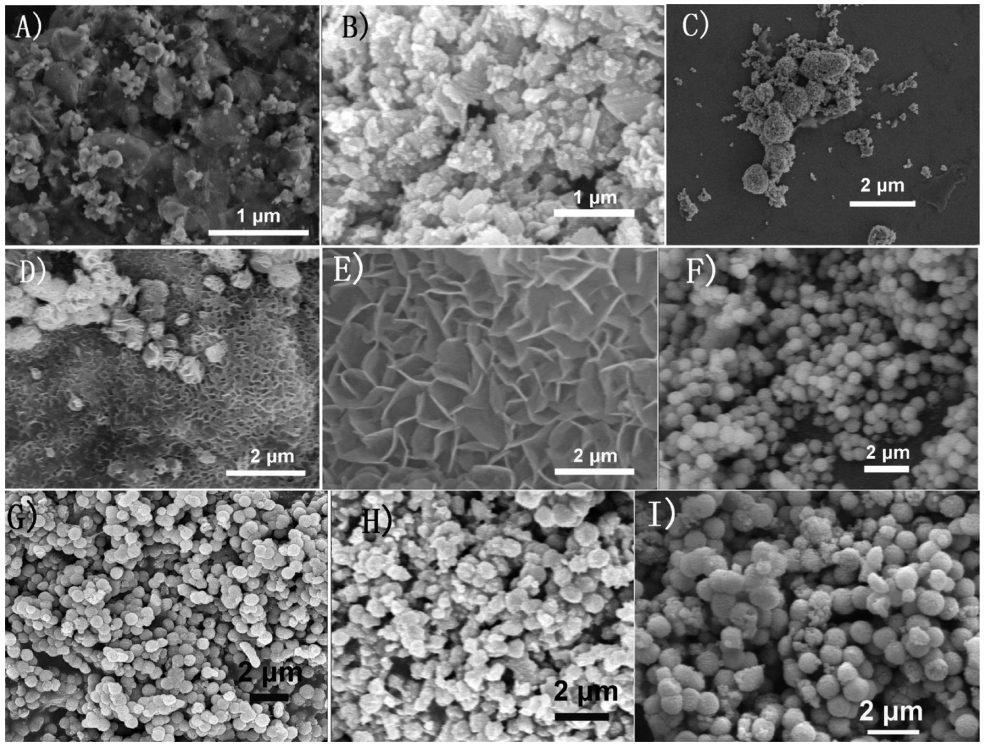

Figure 6. FESEM image of the as-prepared product at 800 °C using, no salt (A); using 30 mmol of NaCl and 10 mmol of KCl (B); using 60 mmol of NaCl and 20 mmol of KCl (C); using 150 mmol of NaCl and 50 mmol of KCl (D); using 180 mmol of NaCl and 60 mmol of KCl (E). The FESEM image of the sample produced by the reaction of 2 mmol of $Fe(NO_3)_3$ and 1 mmol of $Mg(NO_3)_2$ along with 90 mmol of NaCl and 30 mmol of KCl at 760 °C (F); at 860 °C (G); at 900 °C (H). The FESEM image of the sample produced by the reaction of 2 mmol of $Fe(NO_3)_3$ and 1 mmol of $Mg(NO_3)_2$ along with 90 mmol of NaCl and 30 mmol of KCl at 800 °C, the reaction time is 180 min (I).

dx.doi.org/10.1021/ic402558t | *Inorg. Chem.* 2014, 53, 2053−2057

strategy may offer a potential alterative for the synthesis of other nanostructured materials.

AUTHOR INFORMATION

Corresponding Authors

*(Z.L.) Tel.: +86 519 6999842; fax: +86 519 6999516; e-mail: lzs@jstu.edu.cn.

*(C.C.) E-mail: changle@ustc.edu.cn.

Notes

The authors declare no competing financial interest.

ACKNOWLEDGMENTS

This work was supported by the National Natural Science Foundation of China (NSFC 21374108), Natural Science Foundation of Jiangsu Province (BK2010202), Specialized Research Fund for the Doctoral Program of Higher Education of China (20133402120019), the Fundamental Research Funds for the Central Universities (WK2060200012), and the Recruitment Program of Global Experts.

REFERENCES

(1) Deng, H.; Li, X. L.; Peng, Q.; Wang, X.; Chen, J.; Li, Y. D. *Angew. Chem., Int. Ed.* **2005**, *44*, 2782−2785.

(2) Sun, X. P.; Dong, S. J.; Wang, E. K. *J. Am. Chem. Soc.* **2005**, *127*, 13102−13103.

(3) Caruso, F.; Caruso, R. A.; Möhwald, H. *Science* **1998**, *282*, 1111−1114.

(4) Norris, D. J.; Vlaso, Y. A. *Adv. Mater.* **2001**, *13*, 371−376.

(5) Bertino, M. F.; Sun, Z. M.; Zhang, R.; Wang, L. S. *J. Phys. Chem. B* **2006**, *110*, 21416−21418.

(6) Peddis, D.; Cannas, C.; Musinu, A.; Ardu, A.; Orrù, F.; Fiorani, D.; Laureti, S.; Rinaldi, D.; Muscas, G.; Concas, G.; Piccaluga, G. *Chem. Mater.* **2013**, *25*, 2005−2013.

(7) Kamenetzky, E. A.; Mangliocco, L. G.; Pinzer, H. P. *Science* **1994**, *263*, 207−210.

(8) Yi, G. R.; Moon, J. H.; Manoharan, V. N.; Pine, D. J.; Yang, S. M. *J. Am. Chem. Soc.* **2002**, *124*, 13354−13355.

(9) Holtz, J. H.; Asher, S. A. *Nature* **1997**, *389*, 829−832.

(10) Haes, A. J.; Hall, W. P.; Chang, L.; Klein, W. L.; Van Duyune, R. P. *Nano Lett.* **2004**, *4*, 1029−1034.

(11) Kosiorek, A.; Kandulski, W.; Chudzinski, P.; Kempa, K.; Giersig, M. *Nano Lett.* **2004**, *4*, 1359−1363.

(12) Velev, O. D.; Jede, T. A.; Lobo, R. F.; Lenhoff, A. M. *Nature* **1997**, *389*, 447−448.

(13) Yan, F.; Goedel, W. A. *Adv. Mater.* **2004**, *16*, 911−915.

(14) Han, M. G.; Foulger, S. H. *Adv. Mater.* **2004**, *16*, 231−234.

(15) Harold, M. P.; Lee, C.; Burgraaf, A. J.; Keiser, K.; Zaspalis, V. T.; Delange, R. S. A. *MRS Bull.* **1994**, *19*, 34−39.

(16) Bhattacharyya, S.; Salvetat, J. P.; Fleurier, R.; Husmann, A.; Cacciaguerra, T.; Saboungi, M. L. *Chem. Commun.* **2005**, 4818−4820.

(17) Hyeon, T.; Lee, S. S.; Park, J.; Chung, Y.; Na, H. B. *J. Am. Chem. Soc.* **2001**, *123*, 12798−12801.

(18) Xiong, Y.; Xie, X.; Chen, S.; Li, Z. *Chem.—Eur. J.* **2003**, *9*, 4991−4996.

(19) Woo, K.; Lee, H. J.; Ahn, J.; Park, Y. S. *Adv. Mater.* **2003**, *15*, 1761−1764.

(20) Teng, X.; Yang, H. *J. Mater. Chem.* **2004**, *14*, 774−779.

(21) Jun, Y.; Lee, J. H.; Cheon, J. *Angew. Chem., Int. Ed.* **2008**, *47*, 5122−5235.

(22) Park, J.; Joo, J.; Kwon, S.; Jang, Y.; Hyeon, T. *Angew. Chem., Int. Ed.* **2007**, *46*, 4630−4660.

(23) Bárcena, C.; Sra, A. K.; Chaubey, G. S.; Khemtong, C.; Liu, J. P.; Gao, J. *Chem. Commun.* **2008**, 2224−2226.

(24) Bala, T.; Sankar, C. R.; Baidakova, M.; Osipov, V.; Enoki, T.; Joy, P. A.; Prasad, B. L. V.; Sastry, M. *Langmuir* **2005**, *21*, 10638−10643.

(25) Bao, N.; Shen, L.; Wang, Y.; Padhan, P.; Gupta, A. *J. Am. Chem. Soc.* **2007**, *129*, 12374−12375.

(26) Zhang, H.; Qi, R.; Evans, D. G.; Duan, X. *J. Solid State Chem.* **2004**, *177*, 772−780.

(27) Molchanov, V. V.; Buyanov, R. A.; Pavlyukhin, Y. T. *Kinet. Catal.* **2003**, *44*, 788−792.

(28) Liu, Y. L.; Liu, Z. M.; Yang, Y.; Yang, H. F.; Shen, G. L.; Yu, R. Q. *Sens. Actuators B* **2005**, *107*, 600−604.

(29) Darshane, S.; Mulla, I. S. *Mater. Chem. Phys.* **2010**, *119*, 319−323.

(30) Hankare, P. P.; Jadhav, S. D.; Sankpal, U. B.; Patil, R. P.; Sasikala, R.; Mulla, I. S. *J. Alloys Compd.* **2009**, *488*, 270−272.

(31) Bensebaa, F.; Zavaliche, F.; Ecuyer, P. L.; Cochrane, R. W.; Veres, T. *J. Colloid Interface Sci.* **2004**, *277*, 104−110.

(32) Sasakia, T.; Oharaa, S.; Nakaa, T.; Vejpravovab, J.; Sechovskyb, V.; Umetsua, M.; Takamia, S.; Jeyadevanc, B.; Adschiria, T. *J. Supercrit. Fluids* **2010**, *53*, 92−94.

(33) Moumen, N.; Pileni, M. P. *Chem. Mater.* **1996**, *8*, 1128−1134.

(34) Cote, L. J.; Teja, A. S.; Wilkinson, A. P.; Zhang, Z. *Fluid Phase Equilib.* **2003**, *210*, 307−317.

(35) Sun, S. H.; Zeng, H.; Robinson, D. B.; Raoux, S.; Rice, P. M.; Wang, S. X.; Li, G. X. *J. Am. Chem. Soc.* **2004**, *126*, 273−279.

(36) Song, Q.; Zhang, Z. J. *J. Am. Chem. Soc.* **2004**, *126*, 6164−6168.

(37) Wang, X.; Zhuang, J.; Peng, Q.; Li, Y. *Nature* **2005**, *437*, 121−124.

(38) Hayashi, Y.; Kimura, T.; Yamaguchi, T. *J. Mater. Sci.* **1986**, *21*, 757−762.

(39) (a) Liu, X. F.; Fechler, N.; Antonietti, M. *Chem. Soc. Rev.* **2013**, *42*, 8237−8265. (b) Liu, X. F.; Giordano, C.; Antonietti, M. J. *Mater. Chem.* **2012**, *22*, 5454−5459. (c) Liu, X. F.; Giordano, C.; Antonietti, M. *Chem. Mater.* **2013**, *25*, 2021−2027. (d) Duran, C.; Messing, G. L.; Trolier-Mckinstry, S. *Mater. Res. Bull.* **2004**, *39*, 1679−1689.

(40) Dinsmore, A. D.; Hsu, M. F.; Nikolaides, M. G.; Marquez, M.; Bausch, A. R.; Weitz, D. A. *Science* **2002**, *298*, 1006−1009.

(41) Liu, J. J.; Li, F.; Evans, D. G.; Duan, X. *Chem Commun* **2003**, 542−543.

(42) (a) Chandradassa, J.; Jadhava, A. H.; Kimb, K. H.; Kima, H. *J. Alloys Compd.* **2012**, *517*, 164−169. (b) Sun, J. R.; Wang, Z. G.; Wang, Y. Y.; Wei, K. F.; Li, F. S. *Mater. Sci. Forum* **2011**, *686*, 316−319.

(43) Bhardwaj, M. C.; Roy, R. *J. Phys. Chem. Solids* **1971**, *32*, 1603−1607.

(44) Wang, Z. L. *J. Phys. Chem. B* **2000**, *104*, 1153−1175.